Whispering-gallery-mode analysis of phase-matched doubly resonant second-harmonic generation

Yannick Dumeige, Patrice Feron

Whispering-gallery-mode analysis of phase-matched doubly resonant second-harmonic generation

Yannick Dumeige* and Patrice Féron
ENSSAT-FOTON (CNRS-UMR 6082)–Université de Rennes 1, 6 rue de Kerampont, Boîte Postal 80518, 22300 Lannion, France

We propose a coupled modes analysis of second-harmonic generation in microdisk resonators. We demonstrate that whispering gallery modes can be used to obtain a combination of modal and geometrical quasi-phase-matching (without domain inversion) to obtain efficient conversion in isotropic and nonferroelectric materials such as III-V semiconductor compounds. Finally we use an analytical model to describe the coupling between a bus waveguide and the nonlinear microdisk to achieve an optimization scheme for practical configuration.

I. INTRODUCTION

The increase of nonlinear conversion efficiency has been a long-standing goal in nonlinear optics. In the case of second harmonic generation (SHG), different parameters must be considered in order to achieve efficient frequency doubling. A first step to reach this aim consists in choosing materials with large second order nonlinear susceptibility. III-V semiconductors such as $Al_xGa_{1-x}As$ compounds are good candidates for this purpose due to their large nonlinear coefficient d_{14} one order larger than commonly used materials for a fundamental field (FF) wavelength about 1.55 μm [1,2]. The phase matching condition is strictly required to obtain constructive interferences between the nonlinear polarization and the radiated second harmonic (SH) field. This is traditionally obtained using the birefringence of nonlinear materials or more recently, using periodical inversion of the nonlinear susceptibility in ferroelectric materials such as $LiNbO_3$ in order to meet the quasi-phase-matching (QPM) condition [3]. Unfortunately III-V compounds are very dispersive and isotropic around 1.55 μm. Nevertheless, QPM can be implemented at 1.55 μm with different steps of epitaxial growth and technological processes [4,5].

When the phase matching condition is obtained and within the weak conversion limit, doubling efficiency is directly proportional to the FF optical intensity and the square of the interaction length. Waveguiding of SH field and FF can provide high intensity over large lengths leading to an increase in the conversion intensity. In addition, using waveguide properties such as artificial birefringence or modal dispersion permits the phase matching condition to be reached [6,7]. This has already been achieved in AlGaAs waveguides leading to efficient converters [8–10]. Another way to increase the FF intensity consists in embedding the nonlinear material in an external resonant cavity for the FF [11,12]. This can be extended by using a cavity which is also resonant for the SH field [13]. More recently these approaches have been proposed for monolithic microstructured planar devices [14–16] or photonic crystal microcavities [17]. Using epitaxial growth and technology for vertical cavity surface emitting lasers, singly or doubly resonant nonlinear planar III-V semiconductor microcavities with Bragg mirrors have been manufactured [18–20]. These devices pave the way to ultracompact second order nonlinear converters. Although planar approaches are very attractive due to their vertical access, some difficulties inherent in the doubly resonant approach must be circumvented (i) the $\overline{4}3m$ symmetry of AlGaAs compounds, in the commonly used [001] growth direction, gives an effective nonlinear coefficient null under normal incidence, (ii) the strong dispersion of III-V semiconductors around 1.55 μm means that efforts have to be made in design to obtain Bragg mirrors centered around FF and SH frequencies, and (iii) the use of large quality (Q) factor microcavities requires large beam size (in order to limit diffraction effect) leading to a decrease in the FF intensity. The first point is addressed by using large incident angles which can also be used as an external tuning parameters and the second is addressed using aperiodic or high index contrast Bragg mirrors [16,21].

Cylindrical (or spherical) whispering gallery mode (WGM) microcavities working with the total internal reflection (TIR) effect can be used to reach high Q factors. These unique properties have been widely used to achieve low threshold microdisk lasers [22–24]. The use of WGMs in second order nonlinear optics has been less addressed. Schiller and Byer have used monolithic TIR $MgO:LiNbO_3$ resonators to obtain parametric oscillation [25]. Recently Ilchenko *et al.* have used periodically poled $LiNbO_3$ QPM toroidal resonators to efficiently achieve frequency doubling from a wavelength around 1.55 μm [26]. Finally, dispersion of coupled microdisk resonators have been proposed to reach simultaneously quasi phase-matching and enhancement of fields in nonlinear interaction [27,28].

In this paper we propose to use microdisk cavities and their associated WGMs to simultaneously obtain phase matching for III-V semiconductors, FF and SH resonances, and transverse fields confinement. Note that in WGM devices TIR acts as an ultrabroad band mirror working for FF and SH frequencies. This combination could be used to fully integrate nonlinear converters working with low FF power.

The paper is organized as follows. We start with a coupled-mode formulation of the SHG for WGMs in a microdisk. In this second section we review linear properties of WGMs, and we introduce coupled-mode theory (CMT) [29] for SHG in a doubly resonant WGM microcavity. We also

*Electronic address: yannick.dumeige@enssat.fr

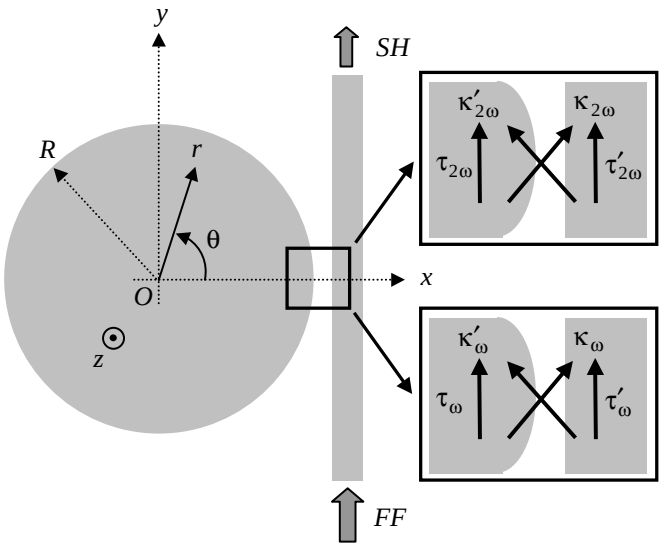

FIG. 1. The generic structure studied in this work is constituted by a nonlinear microdisk side coupled with a bus waveguide. This waveguide allows the insertion of the FF in the waveguide and the extraction of the SH field. τ_ω, τ'_ω, κ_ω, and κ'_ω are the coupling coefficients introduced in Sec. II C.

introduce the coupling with an input/output bus waveguide indispensable for the description of the insertion of the FF in the microdisk and the extraction of the SH field from the microcavity. In the last section, we propose to benefit from the unique properties of WGMs to obtain original phase-matching scheme in III-V semiconductor microdisk. We finish this third section by a discussion of the optimization of coupling between the bus waveguide and the nonlinear microdisk in the perspective of experimental implementation.

II. COUPLED MODE THEORY FOR SHG WITH WGMS

Figure 1 schematizes the cylindrical microcavity studied in this paper. It consists of a microdisk cavity with a second order nonlinear susceptibility $\chi^{(2)}$ coupled to a bus waveguide. This waveguide allows the FF to be inserted in the microcavity and the generated SH field to be extracted from the microcavity. The field confinement in the z direction is provided by planar waveguiding. The required layered structuration is taken into account by the effective index method (EIM) [30]. The refractive index of the nonlinear material at angular frequency ω is $N_\omega=\sqrt{\epsilon_\omega}$, the effective propagation constant associated with the vertical confinement evaluated thanks to the EIM is called $\beta_\omega=n_\omega k_\omega$ where n_ω is the effective index and $k_\omega=\omega/c$ the free space wave vector.

A. Linear properties of WGMs

In the framework of the EIM, the solutions of Maxwell's equations can be divided into two polarized fields TE $(E_z^\omega, H_r^\omega, H_\theta^\omega)$ and TM $(H_z^\omega, E_r^\omega, E_\theta^\omega)$. The fields are all assumed to be CW at single frequency ω for the FF (or 2ω for the SH field). For a microdisk, Ψ^ω represents the electric or the magnetic field depending on the polarization

$$\Psi^\omega(r,\theta,z,t) = \mathcal{A}_\omega \psi^\omega(r)\varphi^\omega(z)e^{j(\omega t-\nu_\omega\theta)}, \tag{1}$$

in the TE case, we can write the magnetic field as

$$\mathbf{H}^\omega(r,\theta,z,t) = \mathcal{A}_\omega \varphi^\omega(z)e^{j(\omega t-\nu_\omega\theta)}(\mathcal{H}_r^\omega\hat{\mathbf{u}}_r + \mathcal{H}_\theta^\omega\hat{\mathbf{u}}_\theta), \tag{2}$$

and in the TM case the electric field is as follows:

$$\mathbf{E}^\omega(r,\theta,z,t) = \mathcal{A}_\omega \varphi^\omega(z)e^{j(\omega t-\nu_\omega\theta)}(\mathcal{E}_r^\omega\hat{\mathbf{u}}_r + \mathcal{E}_\theta^\omega\hat{\mathbf{u}}_\theta). \tag{3}$$

In the TE case $\Psi^\omega=E_z^\omega$, $\psi^\omega=\mathcal{E}_z^\omega$, $\mathcal{H}_r^\omega=\frac{\nu_\omega}{r\mu_0\omega}\psi^\omega$, $\mathcal{H}_\theta^\omega=\frac{1}{j\mu_0\omega}\frac{d\psi^\omega}{dr}$ and in the TM case $\Psi^\omega=H_z^\omega$, $\psi^\omega=\mathcal{H}_z^\omega$, for $r<R$ we have $\mathcal{E}_r^\omega=-\frac{\nu_\omega}{r\epsilon_0 n_\omega^2\omega}\psi^\omega$ and $\mathcal{E}_\theta^\omega=\frac{j}{\epsilon_0 n_\omega^2\omega}\frac{d\psi^\omega}{dr}$, for $r\geqslant R$ we replace n_ω by 1. The integer ν_ω is the azimuthal number. $\varphi^\omega(z)$ is the vertical dependence of the field amplitude and is derived from the solution of the transverse modes in a planar waveguide with the thickness equal to that of the microdisk height. We will consider $\varphi^\omega(z)$ to be dimensionless and harmonic in the nonlinear medium with $|\varphi^\omega(z)|^2=1$. The z component of the wave vector q_ω is deduced from the EIM by: $q_\omega=\sqrt{k_\omega^2N_\omega^2-\beta_\omega^2}$ [31]. Considering these assumptions to be correct, Helmholtz's equation reads

$$\frac{d^2\psi^\omega}{dr^2}+\frac{1}{r}\frac{d\psi^\omega}{dr}+\left(\beta_\omega^2-\frac{\nu_\omega^2}{r^2}\right)\psi^\omega=0. \tag{4}$$

Within the microdisk the solution is described by a Bessel function of the first kind $\psi_\omega(r)=A_\omega J_{\nu_\omega}(\beta_\omega r)$, whereas at the exterior the solution is represented by a Hankel function of the second kind $\psi_\omega(r)=B_\omega H^{(2)}_{\nu_\omega}(k_\omega r)$. Tangential field component continuity allows the link between the constants A_ω and B_ω to be written as follows

$$A_\omega J_{\nu_\omega}(\beta_\omega R) = B_\omega H^{(2)}_{\nu_\omega}(k_\omega R), \tag{5}$$

and the dispersion relation to be calculated using

$$\begin{vmatrix} u_\omega \left.\frac{dJ_{\nu_\omega}}{dr}\right|_{\beta_\omega R} & \left.\frac{dH^{(2)}_{\nu_\omega}}{dr}\right|_{k_\omega R} \\ J_{\nu_\omega}(\beta_\omega R) & H^{(2)}_{\nu_\omega}(k_\omega R) \end{vmatrix} = 0 \tag{6}$$

with $u_\omega=n_\omega$ for TE polarization and $u_\omega=1/n_\omega$ for TM polarization. A_ω is chosen in order to obtain for TE polarization

$$\frac{1}{2}\int_0^{+\infty}(\mathcal{H}_r^\omega)^*\mathcal{E}_z^\omega dr = 1, \tag{7}$$

and for TM polarization

$$-\frac{1}{2}\int_0^{+\infty}(\mathcal{H}_z^\omega)^*\mathcal{E}_r^\omega dr = 1. \tag{8}$$

In these two cases, expression (1) corresponds to an azimuthal power flow of $|\mathcal{A}_\omega|^2 W/m$.

B. Frequency conversion with a nonlinear polarization TE polarized

We adapt the coupled-mode theory developed for planar waveguides [29] for the case of WGMs and thus we start

with Helmholtz's equation in TE polarization

$$\boldsymbol{\nabla}(\boldsymbol{\nabla}\cdot\mathbf{E}^{2\omega})-\Delta\mathbf{E}^{2\omega}=-\mu_0\frac{\partial^2}{\partial t^2}(\epsilon_0\epsilon_{2\omega}\mathbf{E}^{2\omega}+\mathbf{P}), \tag{9}$$

$\mathbf{P}=\epsilon_0\chi^{(2)}:\mathbf{E}^{\omega}\mathbf{E}^{\omega}$ is the second order nonlinear polarization. Taking into account the field dependence given in Eq. (1) and assuming that the FF is TE or TM polarized we have

$$\boldsymbol{\nabla}(\boldsymbol{\nabla}\cdot\mathbf{E}^{2\omega})\cdot\hat{\mathbf{u}}_z=\frac{4q_\omega^2}{\epsilon_0\epsilon_{2\omega}}P_z. \tag{10}$$

Considering only the z component of the electric field, Eq. (9) becomes

$$\Delta_{r,\theta}E_z^{2\omega}+\beta_{2\omega}^2E_z^{2\omega}=-\frac{4(q_\omega^2-\epsilon_{2\omega}k_\omega^2)}{\epsilon_0\epsilon_{2\omega}}P_z, \tag{11}$$

where $\Delta_{r,\theta}$ is the laplacian operator in cylindrical coordinates. Using the slowly varying envelope approximation (SVEA) we can write

$$E_z^{2\omega}(r,\theta,z,t)=\mathcal{A}_{2\omega}(\theta)\mathcal{E}_z^{2\omega}(r)\varphi^{2\omega}(z)e^{j(2\omega t-\nu_{2\omega}\theta)}. \tag{12}$$

Considering only one polarization for the FF:

$$P_z(r,\theta,z,t)=\mathcal{P}_z(r,\theta)[\varphi^{\omega}(z)]^2e^{j(2\omega t-2\nu_\omega\theta)}. \tag{13}$$

Assuming that $[\varphi^{\omega}(z)]^2=\varphi^{2\omega}(z)$ (or $q_{2\omega}=2q_\omega$), which will be the case in the following section since we will only consider the fundamental modes of the planar vertical waveguide, using Eq. (4) and normalization relation (7) for $\mathcal{E}_z^{2\omega}$ we obtain

$$\frac{d\mathcal{A}_{2\omega}}{d\theta}=-\frac{j\beta_{2\omega}^2}{4\nu_{2\omega}\epsilon_0\epsilon_{2\omega}}\left[\int_0^R(\mathcal{H}_r^{2\omega})^*\mathcal{P}_zr^2dr\right]e^{j\Delta\nu\theta}. \tag{14}$$

The integration domain of Eq. (14) is limited to $[0,R]$ since the nonlinear susceptibility vanishes for $r>R$.

C. Linear coupling with the bus waveguide

The imaginary part of the frequencies (ω or 2ω) calculated from Eq. (6) characterizes the intrinsic diffraction losses of the microdisk. In order to take into account all sources of losses (not only diffraction but also surface rugosity for example), using coupled mode theory, and following Rowland and Love [32] it is possible to add losses in the field expression considering the WGM as a bent waveguide mode. The complex frequency or the bent waveguide approaches are equivalent [33]. Consequently we will now consider a complex azimuthal dependence (and a real angular frequency) for the WGM:

$$\tilde{\nu}_\omega=\nu_\omega-j\alpha_\omega R/2, \tag{15}$$

where α_ω represents the overall losses of the WGMs considered as a bent waveguide mode. In order to link the WGMs and the bus waveguide modes we use the matrix approach provided by Yariv in Ref. [34]. Here we consider an asymmetric coupling in order to describe the multimodal behavior of the bus waveguide. Consequently for a given frequency we use four coupling coefficients τ_ω, τ'_ω, κ_ω, and κ'_ω as shematized in Fig. 1:

$$\mathcal{A}_\omega=j\kappa'_\omega\mathcal{A}_{\text{in}}+\tau_\omega\mathcal{A}_\omega e^{-j\tilde{\nu}_\omega 2\pi} \tag{16}$$

assuming a lossless coupling we have $\kappa_\omega^2+\tau_\omega^2=1$, $(\kappa'_\omega)^2+(\tau'_\omega)^2=1$, the power flow of the incoming FF bus waveguide mode is described by $|\mathcal{A}_{\text{in}}|^2$ in the case where only one mode of the bus waveguide is excited. As we want to benefit from resonance field enhancement, we will consider weak coupling and so we assume now (with no loss of generality) that the resonant frequencies of the waveguide-loaded microdisk are the same as the free one [35]. Note that the assumption of a single mode resonator is verified since we consider here only one resonant mode at FF and SH frequencies. The FF envelope is then given by

$$\mathcal{A}_\omega=\frac{j\kappa'_\omega\mathcal{A}_{\text{in}}}{1-\tau_\omega e^{-j\tilde{\nu}_\omega 2\pi}}. \tag{17}$$

We write the same relation as Eq. (16) for the SH field envelope taking into account its angular dependence:

$$\mathcal{A}_{2\omega}(0)=\tau_{2\omega}\mathcal{A}_{2\omega}(2\pi)e^{-j\tilde{\nu}_{2\omega}2\pi}. \tag{18}$$

This last expression combined with Eq. (14) will give us the expression of the SH field generated inside the cavity. With the expression of $\mathcal{A}_{2\omega}(2\pi)$, it is possible to obtain the expression for the SH field radiated out from the cavity through the bus waveguide (for only one mode of the bus waveguide):

$$\mathcal{A}_{\text{out}}=j\kappa_{2\omega}\mathcal{A}_{2\omega}(2\pi)e^{-j\tilde{\nu}_{2\omega}2\pi}. \tag{19}$$

III. APPLICATION TO SHG IN III-V SEMICONDUCTORS

In this section we will apply the formalism developed in Sec. II to the case of highly nonlinear and isotropic III-V semiconductor materials for a FF TM-polarized and an SH TE-polarized field (i.e., parallel to the z direction).

A. Structural description

The proposed structure consists of an etched microdisk made of $Al_{28\%}Ga_{72\%}As$ with a diameter $D=2.1$ μm and a thickness $h=760$ nm (Fig. 2). The chosen Al composition avoids two-photon absorption at FF frequency. The vertical confinement is obtained with a cladding layer of AlAs. This configuration allows the EIM to be used [30]. For convenience, we will call m_i the number of zeros of the considered planar waveguide mode profile along the i direction with $i=\{x,z\}$. At FF wavelength ($\lambda_\omega=1573.4$ nm and $N_\omega=3.2364$) the vertical planar waveguide has two modes whereas at SH wavelength ($N_{2\omega}=3.4632$) three modes can propagate. We have considered here that refractive index of AlAs is 2.9010 at FF frequency and 3.0100 at SH frequency. In the following text we will only consider the fundamental ($m_z=0$) FF and SH modes since the mode coupling (with the same frequency or not) of different orders is weak. The structure can be obtained by epitaxial growth on a GaAs [001]-oriented substrate. The bus waveguide is $t=350$ nm thick, note that this value is always compatible with EIM [30]. This waveguide has two modes indexed by $m_x=0,1$ at FF frequency and has three modes ($m_x=0,1,2$) at SH frequency.

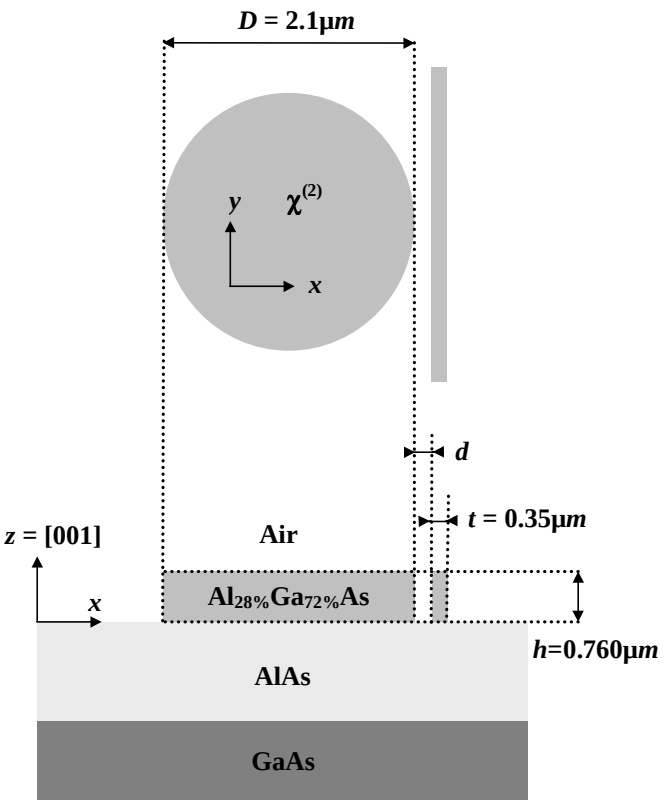

FIG. 2. The proposed structure is etched in a planar waveguide constituted by a core in $Al_{28\%}Ga_{72\%}As$ and a cladding layer in AlAs. The two layers are grown on a GaAs [001]-oriented substrate. The thickness of the microdisk is $h=760$ nm and the distance between the bus waveguide and the microdisk is d. The width of the bus waveguide is $t=350$ nm. The diameter of the microdisk is taken equal to $D=2.1$ μm.

The coupling coefficients between the bus waveguide and the microdisk depend on the value of the gap d between the microdisk and the bus waveguide. Taking into account the strong natural dispersion of AlGaAs, these design parameters allow the azimuthal numbers $\nu_\omega=9$ and $n=1$ for the FF; $\nu_{2\omega}=20$ and $n=2$ for the SH field to be obtained (where n is the number of maxima of the radial dependence of the intensity). Because of the very strong dispersion of AlGaAs at $\lambda_\omega=1573.4$ nm, it remains a phase mismatch $\Delta\nu=\nu_{2\omega}-2\nu_\omega=2$ (note that we also have $\Delta\tilde{\nu}=\tilde{\nu}_{2\omega}-2\tilde{\nu}_\omega$). We will see in the following section that this phase mismatch will be compensated for using the unique properties of WGMs.

B. Phase-matching consideration

The cubic $\bar{4}3m$ symmetry of AlGaAs and the TM polarization for the FF leads to the following expression for nonlinear polarization [36]:

$$\mathcal{P}_z = 2\epsilon_0 d_{14}\mathcal{A}_\omega^2 \mathcal{E}_x^\omega \mathcal{E}_y^\omega, \tag{20}$$

where $d_{14}=108$ pm/V for the chosen Al composition [1,2]. In the cylindrical coordinates the nonlinear polarization reads

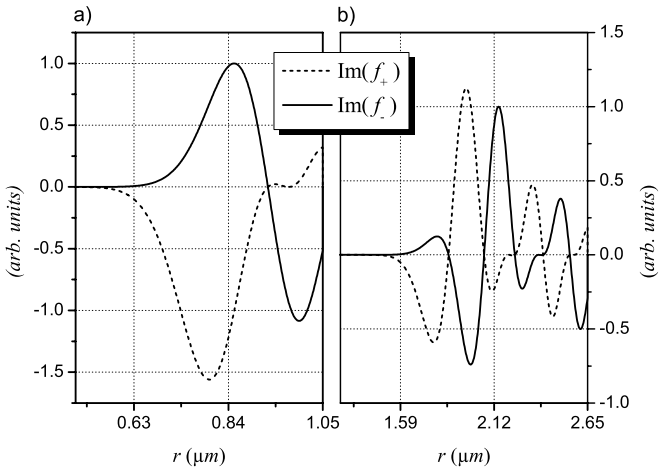

FIG. 3. Functions $\mathrm{Im}(f_+)$ (dash lines) and $\mathrm{Im}(f_-)$ (full lines) normalized for the maximal value of $\mathrm{Im}(f_-)$ as a function of r inside the microdisk: (a) for the proposed structure with $D=2.1$ μm, (b) for the same structure with $D=5.3$ μm, $n=2$ for the FF and $n=5$ for the SH field. In this last case, we have for the phase mismatch $\Delta\nu=44-2\times23=-2$.

$$\mathcal{P}_z = \epsilon_0 d_{14}\mathcal{A}_\omega^2\{2\mathcal{E}_r^\omega\mathcal{E}_\theta^\omega\cos(2\theta) + [(\mathcal{E}_r^\omega)^2 - (\mathcal{E}_\theta^\omega)^2]\sin(2\theta)\}. \tag{21}$$

This leads to the following angular dependence for the effective nonlinear polarization

$$\int_0^R (\mathcal{H}_r^{2\omega})^* \mathcal{P}_z r^2 dr = \mathcal{A}_\omega^2 (a_+ e^{2j\theta} + a_- e^{-2j\theta}). \tag{22}$$

This natural modulation of the nonlinear tensor can be used to reach the quasi-phase-matching condition. Taking into account this feature (14) reads

$$\frac{d\mathcal{A}_{2\omega}}{d\theta} = -\frac{j\beta_{2\omega}^2\mathcal{A}_\omega^2}{4\nu_{2\omega}\epsilon_0\epsilon_{2\omega}}[a_+ e^{j(\Delta\tilde{\nu}+2)\theta} + a_- e^{j(\Delta\tilde{\nu}-2)\theta}]. \tag{23}$$

In order to analyze the SH field and nonlinear polarization overlap we define

$$a_\pm = \int_0^R f_\pm(r) dr, \tag{24}$$

with

$$f_\pm(r) = \epsilon_0 r^2 d_{14}(\mathcal{H}_r^{2\omega})^* \left\{ \mathcal{E}_r^\omega\mathcal{E}_\theta^\omega \pm \frac{j}{2}[(\mathcal{E}_\theta^\omega)^2 - (\mathcal{E}_r^\omega)^2] \right\}, \tag{25}$$

which is an imaginary quantity. Figure 3(a) shows $\mathrm{Im}(f_+)$ and $\mathrm{Im}(f_-)$ for the structure already described. We can notice that due to a weak overlap between the nonlinear polarization and the SH field $|a_-|$ is lower than $|a_+|$, calculations show that $|a_+/a_-|\approx 6$. Unfortunately regarding the strong material and structural dispersions, it is not possible to obtain $\Delta\nu=-2$ for low value of n for FF and SH field which could lead to phase match the term in a_+ and to a better overlap between the nonlinear polarization and the SH field. It is possible to obtain the condition $\Delta\nu=-2$ with high values of n both at FF and SH wavelengths. In Fig. 3(b) we represent

$\mathrm{Im}(f_+)$ and $\mathrm{Im}(f_-)$ for a the same structure as described in Fig. 2 but with D=5.3 μm, λ_ω=1578.5 nm, n=2 for FF and n=5 for SH. In this case $\Delta\nu$=44−2×23=−2 and $|a_+/a_-|\approx 3$. Although the effective nonlinear susceptibility is better than in the precedent case, we did not study this structure since high values of n increase the WGMs volume which is detrimental for nonlinear interactions.

In the case chosen here and described in Sec. II, we have $\Delta\nu$=2, so only the term in a_- is phase matched, consequently,

$$\mathcal{A}_{2\omega}(2\pi) - \mathcal{A}_{2\omega}(0) = -\frac{j\beta_{2\omega}^2 \mathcal{A}_\omega^2 a_-}{2\nu_{2\omega}\epsilon_0\epsilon_{2\omega}} \frac{e^{(\alpha_{2\omega}-2\alpha_\omega)\pi R}-1}{(\alpha_{2\omega}-2\alpha_\omega)R}. \tag{26}$$

If we define

$$\tilde{K} = -\frac{j\beta_{2\omega}^2 a_-}{2\nu_{2\omega}\epsilon_0\epsilon_{2\omega}} \frac{e^{(\alpha_{2\omega}-2\alpha_\omega)\pi R}-1}{(\alpha_{2\omega}-2\alpha_\omega)R}, \tag{27}$$

we can write the expression for the SH field generated inside the cavity as

$$\mathcal{A}_{2\omega}(2\pi) = \frac{\tilde{K}\mathcal{A}_\omega^2}{1-\tau_{2\omega}e^{-j\tilde{\nu}_{2\omega}2\pi}}. \tag{28}$$

We can now obtain the expression of the conversion efficiency η:

$$\eta = \left|\frac{\mathcal{A}_{\mathrm{out}}}{\mathcal{A}_{\mathrm{in}}}\right|^2 = \frac{(\kappa_{2\omega})^2(\kappa'_\omega)^4|\tilde{K}|^2|\mathcal{A}_{\mathrm{in}}|^2 e^{-\alpha_{2\omega}2\pi R}}{|1-\tau_\omega e^{-j\tilde{\nu}_\omega 2\pi}|^4 |1-\tau_{2\omega}e^{-j\tilde{\nu}_{2\omega}2\pi}|^2}, \tag{29}$$

which shows good agreement with the expression given in Ref. [15] for a planar monolithic microcavity.

C. FF and SH field impedance matching

Equation (29) should be written for each mode of the bus waveguide at SH frequency. We have already emphasized that this waveguide has several modes at FF and SH frequencies. We still consider uniquely the fundamental (m_z=0) even mode in the vertical direction for the FF and SH fields since the resonant modes inside the microcavity have m_z=0 and will couple preferentially with a same order mode. In order to take into account the different modes with x-dependent profiles (m_x=0,1,2) we will link the coupling coefficients to the external quality factor and derive an expression of the conversion efficiency as a function of Q factors (in this case $\mathcal{A}_{\mathrm{out}}$ is the overall power flow corresponding to the generated SH field). Since the external quality factors which take the multimodal behavior of the bus waveguide into account can be calculated analytically as a function of d [37], this will give us a physical insight into the impact of d on the conversion efficiency. Taking into account that ν_ω is an integer, Eq. (29) can be written

$$\eta = \frac{(\kappa_{2\omega})^2(\kappa'_\omega)^4|K|^2|\mathcal{A}_{\mathrm{in}}|^2 e^{-\alpha_{2\omega}2\pi R}}{(1-\tau_\omega e^{-\alpha_\omega \pi R})^4 (1-\tau_{2\omega}e^{-\alpha_{2\omega}\pi R})^2}. \tag{30}$$

Carrying out the high finesse cavity approximation we can write that $\tau_\omega \approx 1$ and

$$1-\tau_\omega e^{-\alpha_\omega \pi R} \approx 1-\tau_\omega+\alpha_\omega \pi R. \tag{31}$$

It is possible to link these parameters to Q factors [38]. With this objective in mind, we define the internal quality factor as

$$Q_\omega^0 = \frac{2\pi N_\omega}{\alpha_\omega \lambda_\omega} \tag{32}$$

and the external quality factors as

$$Q_\omega^e = \frac{\pi\nu_\omega}{1-\tau_\omega}, \quad Q_\omega^{e\prime} = \frac{\pi\nu_\omega}{1-\tau'_\omega}. \tag{33}$$

We can write the expression of the conversion efficiency as a function of quality factors for the FF and the SH field:

$$\eta \approx \frac{8|K|^2|\mathcal{A}_{\mathrm{in}}|^2}{\pi^3 {\nu_\omega}^2 \nu_{2\omega}(Q_\omega^{e\prime})^2} \times \frac{(Q_\omega^e)^4 Q_{2\omega}^e e^{-4\pi^2 N_{2\omega}R/(\lambda_{2\omega}Q_{2\omega}^0)}}{\left(1+\frac{2\pi N_\omega R}{\lambda_\omega \nu_\omega}\frac{Q_\omega^e}{Q_\omega^0}\right)^4 \left(1+\frac{2\pi N_{2\omega}R}{\lambda_{2\omega}\nu_{2\omega}}\frac{Q_{2\omega}^e}{Q_{2\omega}^0}\right)^2}, \tag{34}$$

where $|K|^2$ is the first order development of $|\tilde{K}|^2$ in $(\alpha_{2\omega}-2\alpha_\omega)\,R$:

$$K = -\frac{\pi j\beta_{2\omega}^2 a_-}{2\nu_{2\omega}\epsilon_0\epsilon_{2\omega}}. \tag{35}$$

Using the following crude approximation:

$$\nu_\omega \approx \frac{2\pi}{\lambda_\omega} N_\omega R, \tag{36}$$

we can generalize the result of Di Falco *et al.* [17] and write

$$\eta \approx \frac{8|K|^2|\mathcal{A}_{\mathrm{in}}|^2}{\pi^3 {\nu_\omega}^2 \nu_{2\omega}} \frac{(Q_\omega^e)^4 Q_{2\omega}^e e^{-2\pi\nu_{2\omega}/Q_{2\omega}^0}}{(Q_\omega^{e\prime})^2 \left(1+\frac{Q_\omega^e}{Q_\omega^0}\right)^4 \left(1+\frac{Q_{2\omega}^e}{Q_{2\omega}^0}\right)^2}. \tag{37}$$

Depending on the relative values of Q_ω^0 and Q_ω^e (and obviously the relative values of $Q_{2\omega}^0$ and $Q_{2\omega}^e$), the conversion efficiency can be greatly enhanced or decreased. We used the analytical model proposed by Morand *et al.* in Ref. [37] to evaluate Q_ω^e for the different modes of the bus waveguide and the two frequencies as a function of d. Following Ref. [37], we now present the expression of the intrinsic Q factor (i.e., only limited by diffraction and external coupling) Q_ω^{int} for a microdisk waveguide side coupled without internal losses [37]

$$\frac{1}{Q_\omega^{\mathrm{int}}} = \frac{1}{Q_\omega^{\mathrm{diff}}}\left(1+\frac{P_\omega^G}{P_\omega^{\mathrm{rad}}}\right), \tag{38}$$

where Q_ω^{diff} is the Q factor diffraction limited, P_ω^G the power carried by the waveguide and P_ω^{rad} the power radiated outside the microdisk for a given polarization. Note that here we calculate the value of Q_ω^{diff} by

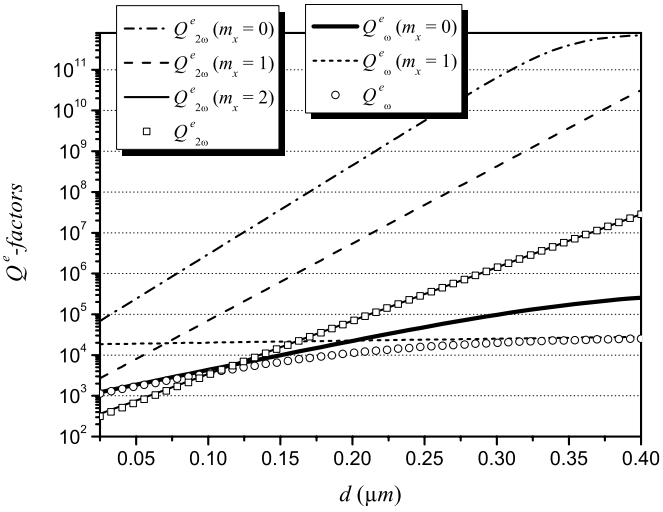

FIG. 4. External Q factors as a function of distance between the microdisk and the bus waveguide d. For FF frequency $Q^e_\omega(m_x)$ is represented for the two possible modes ($m_x=0,1$), for SH, frequency $Q^e_{2\omega}(m_x)$ is represented for the three possible modes ($m_x=0,1,2$). The overall values Q^e_ω and $Q^e_{2\omega}$ are also shown (white circles and squares, respectively).

$$Q^{\text{diff}}_\omega = \frac{\omega E^{\text{inside}}_\omega}{P^{\text{rad}}_\omega}, \tag{39}$$

where E^{inside}_ω is the energy stored in the microdisk, see [37]. Since Q^{diff}_ω is always very large, we will consider that $Q^e_\omega = Q^{\text{int}}_\omega$. We can calculate $P^G_\omega(m_x)$ for the different modes and for the two frequencies we link the overall external Q factor Q^e_ω to the external Q factors calculated for each mode $Q^e_\omega(m_x)$:

$$\frac{1}{Q^e_\omega} = \sum_{m_x=0}^{s_\omega} \frac{1}{Q^e_\omega(m_x)} \tag{40}$$

with $s_\omega=2$ and $s_{2\omega}=3$. We will consider here that the incoming FF mode corresponds to $m_x=0$ so we have $Q^{e\prime}_\omega = Q^e_\omega(m_x=0)$ since κ'_ω corresponds to the coupling coefficient from the fundamental mode ($m_z=0$) of the bus waveguide to the FF WGM. Otherwise, Q^e_ω takes into account the two modes of the bus waveguide since the resonant FF can escape from the microcavity coupling with these two modes. Figure 4 represents $Q^e_\omega(m_x)$ and $Q^e_{2\omega}(m_x)$ [calculated from Eq. (38)] as a function of d. First, we can notice that for $m_x=0$ the fields are well confined both at FF and SH frequencies and Q^e_ω reach their intrinsic limits Q^{diff}_ω for $d \geqslant 400$ nm. As expected, Q^e_ω increase with d because the evanescent coupling also increases. In the case of FF, $Q^e_\omega(m_x=0) > Q^e_\omega(m_x=1)$ for large values of d since the confinement is weaker for $m_x=1$ than for $m_x=0$. For low values of d, even the mode with $m_x=1$ is less confined than the fundamental mode ($m_x=0$), we have $Q^e_\omega(m_x=0) < Q^e_\omega(m_x=1)$. This can be attributed to the large propagation constant mismatch between the mode indexed by $m_x=1$ and the FF WGM. The overall values Q^e_ω (white circles) and $Q^e_{2\omega}$ (white squares) are also represented. We can notice that $Q^e_{2\omega} \approx Q^e_{2\omega}(m_x=2)$ for all the values of d since

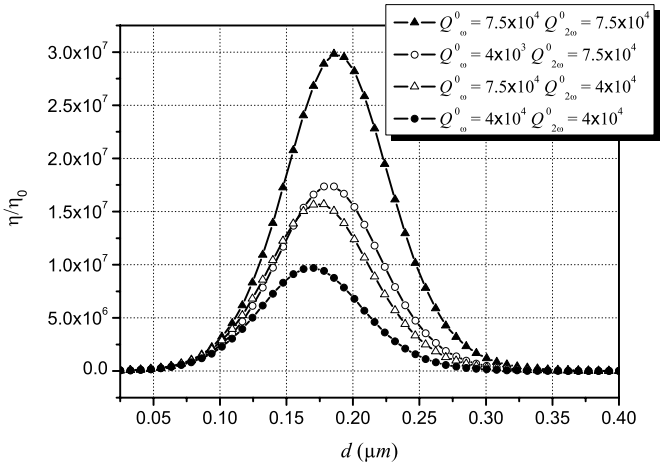

FIG. 5. Enhancement factor η/η_0 as a function of the distance between the bus waveguide and the microdisk calculated for different values $(Q^0_\omega, Q^0_{2\omega})$ of internal Q factors: (i) solid triangles $(7.5\times10^4, 7.5\times10^4)$, (ii) white circles $(4\times10^4, 7.5\times10^4)$, (iii) white triangles $(7.5\times10^4, 4\times10^4)$, (iv) solid circles $(4\times10^4, 4\times10^4)$.

$$Q^e_{2\omega}(m_x=2) \lll Q^e_{2\omega}(m_x=1) \lll Q^e_{2\omega}(m_x=0). \tag{41}$$

It is then possible to calculate the value of η/η_0 as a function of d (Fig. 5) using Eq. (34) and considering

$$\eta_0 = |K|^2 |\mathcal{A}_{\text{in}}|^2. \tag{42}$$

The ratio η/η_0 represents the enhancement factor due to the double resonance for different values of internal losses or internal quality factors at FF and SH field frequencies. We can see that the conversion efficiency can reach an optimal value depending on the internal losses. This demonstrates that from a practical point of view, an optimal coupling can be chosen for given overall losses. Defining the overall Q factor Q_ω as

$$\frac{1}{Q_\omega} = \frac{1}{Q^e_\omega} + \frac{1}{Q^0_\omega}, \tag{43}$$

in the case of $Q^0_{2\omega} = Q^0_\omega = 7.5\times10^4$ (values compatible with recent achievements of AlGaAs microdisks [24]), we obtain an optimal coupling distance $d \approx 185$ nm, $Q_\omega \approx 8700$ and $Q_{2\omega} \approx 28\,000$, this gives us a conversion efficiency equal to 1% for an external FF power of 130 μW and a vertical FF mode thickness equal to h [39].

IV. CONCLUSION

We have derived CMT for SHG in microdisk resonators adapting the results of Ref. [29] to the case of WGMs. We also proposed a simple way to achieve combination of modal and quasi-phase-matching in WGM resonators. This can be applied to the case of isotropic III-V semiconductors grown along the commonly used [001] crystallographic direction combining the advantages of resonant fields enhancement and waveguiding fields confinement. We would like to emphasize the crucial role of the coupling between the microdisk and the bus waveguide and overall optical losses. An

external tuning parameter (such as temperature, for example) will have to be found to reach experimentally the double resonance condition as it is done with the incident angle in the vertical access approach [16,19]. When this condition will be fulfilled, this configuration could be used to obtain micron-size integrated parametric devices such as converters or generators. Second order nonlinear microdisk coupled with waveguides could be used to integrate the all-optical processing function proposed by Cojocaru *et al.* [40]. Adaptation of this approach to materials grown on InP could present the possibility of monolithic integration with communication lasers at 1.3 and 1.55 μm [41].

ACKNOWLEDGMENTS

This work was backed by French "Agence Nationale de la Recherche" through the project O^2E (Grant No. NT05-3-45032). We wish to thank S. Bodros for her help in preparing the manuscript.

[1] M. Ohashi, T. Kondo, R. Ito, S. Fukatsu, Y. Shiraki, K. Kumata, and S. S. Kano, J. Appl. Phys. **74**, 596 (1993).
[2] I. Shoji, T. Kondo, A. Kitamoto, M. Shirane, and R. Ito, J. Opt. Soc. Am. B **14**, 2268 (1997).
[3] M. M. Fejer, G. A. Magel, D. H. Jundt, and R. L. Byer, IEEE J. Quantum Electron. **28**, 2631 (1992).
[4] S. J. B. Yoo, R. Bhat, C. Caneau, and M. A. Koza, Appl. Phys. Lett. **66**, 3410 (1995).
[5] J. S. Aitchison, M. W. Street, N. D. Whitbread, D. C. Hutchings, J. H. Marsh, G. T. Kennedy, and W. Sibbett, IEEE J. Sel. Top. Quantum Electron. **4**, 695 (1998).
[6] J. P. van der Ziel, Appl. Phys. Lett. **26**, 60 (1975).
[7] B. Oster and H. Fouckhardt, Appl. Phys. B: Lasers Opt. **73**, 535 (2001).
[8] A. Fiore, V. Berger, E. Rosencher, P. Bravetti, and J. Nagle, Nature (London) **391**, 463 (1998).
[9] A. Fiore, S. Janz, L. Delobel, P. van der Meer, P. Bravetti, V. Berger, E. Rosencher, and J. Nagle, Appl. Phys. Lett. **72**, 2942 (1998).
[10] S. Ducci, L. Lanco, V. Berger, A. De Rossi, V. Ortiz, and M. Calligaro, Appl. Phys. Lett. **84**, 2974 (2004).
[11] J. A. Armstrong, N. Bloembergen, J. Ducuing, and P. S. Pershan, Phys. Rev. **127**, 1918 (1962).
[12] A. Ashkin, G. D. Boyd, and J. M. Dziedzic, IEEE J. Quantum Electron. **2**, 109 (1966).
[13] Z. H. Ou and H. J. Kimble, Opt. Lett. **18**, 1053 (1993).
[14] E. Rosencher, B. Vinter, and V. Berger, J. Appl. Phys. **78**, 6042 (1995).
[15] V. Berger, J. Opt. Soc. Am. B **14**, 1351 (1997).
[16] M. Liscidini and L. C. Andreani, Phys. Rev. E **73**, 016613 (2006).
[17] A. Di Falco, C. Conti, and G. Assanto, Opt. Lett. **31**, 250 (2006).
[18] S. Nakagawa, N. Yamada, N. Mikoshiba, and D. E. Mars, Appl. Phys. Lett. **66**, 2159 (1995).
[19] C. Simonneau, J. P. Debray, J. C. Harmand, P. Vidaković, D. J. Lovering, and J. A. Levenson, Opt. Lett. **22**, 1775 (1997).
[20] X. Mu, Y. J. Ding, H. Yang, and G. J. Salamo, Appl. Phys. Lett. **79**, 569 (2001).
[21] D. J. Lovering, G. Fino, C. Simonneau, R. Kuszelewicz, R. Azoulay, and J. A. Levenson, Electron. Lett. **32**, 1782 (1996).
[22] S. L. McCall, A. F. J. Levi, R. E. Slusher, S. J. Pearton, and R. A. Logan, Appl. Phys. Lett. **60**, 289 (1992).
[23] M. Fujita, R. Ushigome, and T. Baba, Electron. Lett. **34**, 278 (2000).
[24] K. Srinivasan, M. Borselli, O. Painter, A. Stintz, and S. Krishna, Opt. Express **14**, 1094 (2006).
[25] S. Schiller and R. L. Byer, J. Opt. Soc. Am. B **10**, 1696 (1993).
[26] V. S. Ilchenko, A. A. Savchenkov, A. B. Matsko, and L. Maleki, Phys. Rev. Lett. **92**, 043903 (2004).
[27] Y. Xu, R. K. Lee, and A. Yariv, J. Opt. Soc. Am. B **17**, 387 (2000).
[28] S. Mookherjea and A. Yariv, Phys. Rev. E **65**, 026607 (2002).
[29] A. Yariv, IEEE J. Quantum Electron. **9**, 919 (1973).
[30] M. K. Chin and S. T. Ho, J. Lightwave Technol. **16**, 1433 (1998).
[31] K. Phan Huy, A. Morand, and P. Benech, IEEE J. Quantum Electron. **41**, 357 (2005).
[32] D. R. Rowland and J. D. Love, IEE Proc.: Optoelectron. **140**, 177 (1993).
[33] L. Prkna, J. Čtyroký, and M. Hubálek, Opt. Quantum Electron. **36**, 259 (2004).
[34] A. Yariv, Electron. Lett. **36**, 321 (2000).
[35] K. Hiremath, Ph.D. thesis, University of Twente, The Netherlands, 2005.
[36] P. N. Butcher and D. Cotter, *The Elements of Nonlinear Optics* (Cambridge University Press, Cambridge, 1990).
[37] A. Morand, K. Phan Huy, Y. Desières, and P. Benech, J. Lightwave Technol. **22**, 827 (2004).
[38] M. Rosenblit, P. Horak, S. Helsby, and R. Folman, Phys. Rev. A **70**, 053808 (2004).
[39] E. Rosencher and B. Vinter, *Optoelectronics* (Cambridge University Press, New York, 2002).
[40] C. Cojocaru, J. Martorell, R. Vilaseca, J. Trull, and E. Fazio, Appl. Phys. Lett. **74**, 504 (1999).
[41] M. Cada, M. Svilans, S. Janz, R. Bierman, R. Normandin, and J. Glinski, Appl. Phys. Lett. **61**, 2090 (1992).